

Microwave absorption at low magnetic field in sintered $\text{YBa}_2\text{Cu}_3\text{O}_7$: Freezing effects at low temperature and superconducting-glass model

M. Giura, R. Marcon, and R. Fastampa

*Dipartimento di Fisica Università di Roma "La Sapienza" Piazzale A. Moro, 2 I-00185 Roma, Italy;
Gruppo Nazionale di Struttura della Materia del Consiglio Nazionale delle Ricerche, Roma, Italy;
and Centro Interuniversitario di Struttura della Materia del Ministero della Pubblica Istruzione, Roma, Italy*
(Received 23 January 1989)

The Josephson-junction (JJ) model in $\text{YBa}_2\text{Cu}_3\text{O}_7$ sintered samples is confirmed by means of microwave absorption measurements at low magnetic field (< 500 G). An explanation of measures supporting the JJ model is given. At low temperature (< 7 K) experimental evidence shows that the array of junctions is driven by the magnetic field in a frozen state. A qualitative interpretation of this effect in the frame of the superconducting-glass picture is presented.

I. INTRODUCTION

Since the discovery of high- T_c superconducting copper oxide compounds,¹ measurements have been carried out to investigate the magnetic properties both in sintered and in single-crystal samples. Measurements of magnetization, susceptibility, and microwave absorption on sintered samples have suggested the existence of superconducting domains coupled via the proximity effect or Josephson tunneling.²⁻⁴ Measurements of magnetic relaxation, dc resistivity, and magnetic torque have shown effects of flux pinning and dissipation due to flux creep such as in type-II superconductors.⁵⁻⁶

Microwave absorption turned out to be a powerful tool for studying the magnetic properties of high- T_c superconductors. In the literature this type of measurement has usually been performed by means of an EPR spectrometer, which gives the derivative in the magnetic field of the absorbed microwave power. Our measurements are based on a boxcar technique which directly detects the microwave absorption. By using this technique, it is possible to distinguish between an exponential-like behavior at low fields ($H < 500$ G) and a linear one at higher fields. An analysis of the two behaviors as a function of temperature allows us to say that they refer to different phenomena. In a previous work⁷ the exponential behavior has been related to the presence of Josephson junctions. In particular the existence of a critical temperature $T_{cj} < T_{c0}$ (with T_{c0} superconducting transition temperature of the sample) below which the exponential behavior disappears was found. Our experimental results are directly comparable with the EPR "spectra." Referring to work of Glarum *et al.*,⁸ we can say that the absorption peak at low fields is the derivative of our exponential behavior. They show that this peak disappears at a temperature below T_{c0} ; besides, near T_{c0} a step is present close to $H=0$, integration giving our linear dependence. The presence of thermal activation effects and the connection with the critical field H_{c2} , suggest an interpretation in terms of the flux creep of this linear dependence, as will be shown in another paper. This is in

agreement with recent measurements of magnetic relaxation, dc resistivity, and critical current near T_{c0} .⁵

In the present work new experimental results in $\text{YBa}_2\text{Cu}_3\text{O}_7$ and a more accurate elaboration of the whole set of measures at low fields supporting the Josephson-junction (JJ) model are presented. We consider a network of independent junctions with statistically distributed geometrical parameters. Assuming a decoupling probability of the single junction exponentially depending on H , it is possible to explain the behaviors of (i) the microwave absorbed power $P(H)$ as a function of H , (ii) the maximum absorbed power ΔP_0 versus T , and (iii) the mean dephasing magnetic field of junctions H_d versus T . At low temperature (< 45 K) the single-junction model is not able to explain the metastability effects which make H_d dependent on the magnetic history of the sample. In particular, at very low temperature (< 7 K) experimental evidence shows that the system of junctions is driven by the magnetic field in a frozen state, from which it can be removed only by heating the sample at higher temperature. Therefore we give a qualitative interpretation of this fact in the framework of the superconducting-glass (SG) picture.⁹⁻¹² In Sec. II we present the experimental results, in Sec. III a microwave absorption model at a low magnetic field is exposed, while in Sec. IV the SG interpretation for low-temperature measurements is given.

II. EXPERIMENTAL RESULTS

The experimental setup has been reported in a previous paper.⁴ The results refer to the absorption of the microwave power $P(H)$ in sintered samples of $\text{YBa}_2\text{Cu}_3\text{O}_7$, at 23 GHz as a function of the magnetic field H up to 3 kG in the temperature range 2–100 K. The samples, disk shaped (diameter 13 mm, thickness 3 mm), are the bottom of a cylindrical resonant cavity tuned in the TE_{011} mode. Measurements are carried out with a dc technique by means of a boxcar integrator.

Typical behaviors of $P(H)$ are shown in Fig. 1 for different temperatures. The dependence of $P(H)$ on H

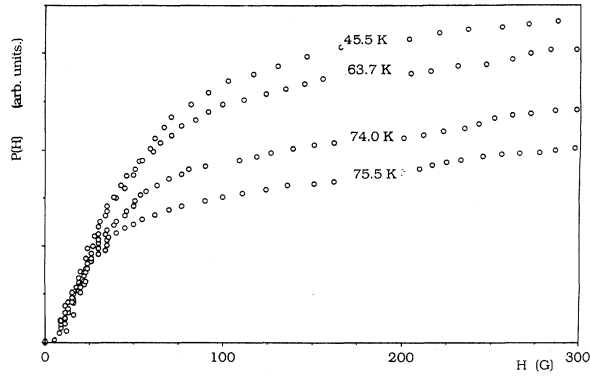


FIG. 1. Microwave absorbed power $P(H)$ as a function of the external magnetic field H at various temperatures.

can be considered the superposition of a linear part present up to high fields (~ 10 kG) and an exponential-like one at low fields, as was already shown in Ref. 7 [from now on referred to as (I)]. The linear behavior is present in the whole range of temperature, up to the sample transition temperature T_{c0} (91.5 K). The exponential-like part disappears at a temperature T_{cj} well below T_{c0} . These results suggest that the two behaviors refer to different physical effects. In this paper, since we are interested in the low-field exponential behavior, we subtract the linear part from the curves of Fig. 1, obtaining the points $\tilde{P}(H)$ of Fig. 2. The amplitude ΔP_0 of the effect, defined as

$$\Delta P_0 = \tilde{P}(\infty) - \tilde{P}(0),$$

is varying with the temperature T and vanishes before reaching T_{c0} , as can be seen in Fig. 3, where the behavior (dots) of ΔP_0 versus T is reported. As it will be shown in Sec. III. B, it is possible to extrapolate a temperature T_{cj} , below T_{c0} , at which ΔP_0 goes to zero.

Moreover, metastability effects are present in the mea-

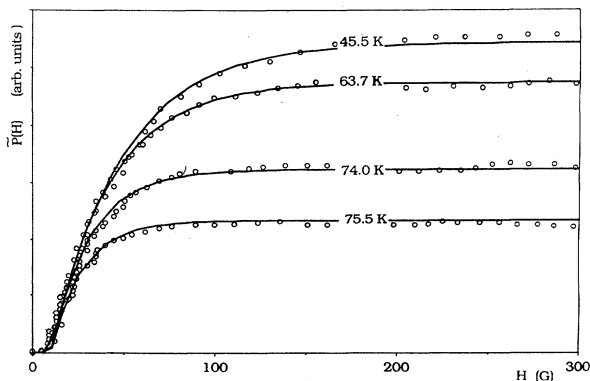


FIG. 2. Points refer to the absorbed power $\tilde{P}(H)$ of Fig. 1 when the linear part is subtracted. Continuous lines are the fit curves carried out by the procedure of Sec. III A.

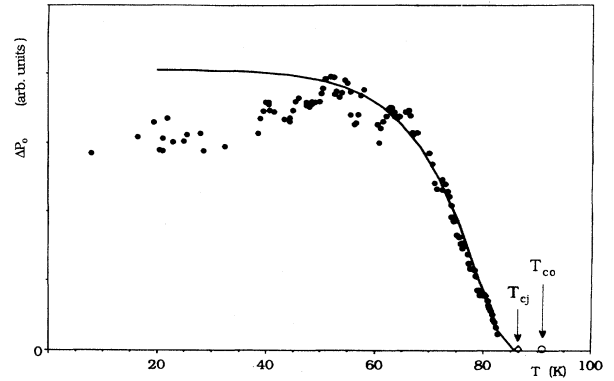


FIG. 3. Maximum variation $\Delta P_0 = \tilde{P}(\infty) - \tilde{P}(0)$ of the absorbed power $\tilde{P}(H)$ of Fig. 2 as a function of the temperature. Dots refer to experimental results, the solid line refers to the fit curve obtained in a single-junction model (Sec. III B). Fit parameters are $w = 1.6 \mu\text{m}$, $l = 0.01 \mu\text{m}$, $\lambda_0 = 0.1 \mu\text{m}$, and $\sigma = 0.28 \mu\text{m}$.

surements below 45 K. In particular at 2.3 K, after the first run after a zero-field cooling (ZFC), where the typical behavior $P(H)$ of Fig. 1 is present (curve *a* of Fig. 4), the effect is no more detectable if the field H in the first run was driven up to 1 kG (curve *b* of Fig. 4). It is possible to again obtain the curve *A* only if the sample is first heated up to ~ 45 K and then again cooled at 2.3 K.

III. ABSORPTION MODEL AT LOW MAGNETIC FIELDS

As we have already shown in paper (I) the low-field behavior of the microwave absorbed power is connected to the presence of Josephson junctions. The experimental evidence of a well-defined critical temperature T_{cj} ($< T_{c0}$) and the metastability effects suggest that the more acceptable model is that of arrays of junctions, as it

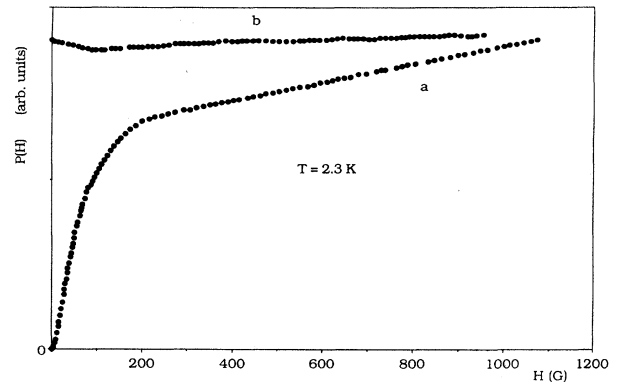


FIG. 4. Absorbed power $P(H)$, as in Fig. 1, at $T = 2.3$ K. Curve *a* refers to the first run in a magnetic field after ZFC. Curve *b* refers to a successive run, when H in the first run ranged above 1 kG. One can again obtain the behavior (*a*) only if the sample is heated above ~ 45 K.

will be seen in Sec. IV. However, at high temperature (> 45 K) an independent single-junction model is able to explain the experimental results.

The variation $\tilde{P}(H)$ (Fig. 2) is due to the magnetic decoupling of junctions that makes the rf current dissipative across the broken junctions. We assume (i) an independent junction model and that (ii) the relative variation of the number of coupled junctions is proportional to the magnetic field variation. It is equivalent to suppose that the probability of finding a junction still coupled at a field H is proportional to

$$\exp[-(H-H_1)/H_d]$$

for $H > H_1$, where H_1 is the value above which the magnetic field penetrates into the junction, and H_d is the mean field of decoupling.

A. Calculation of the microwave absorbed power $P(H)$ as a function of the magnetic field H

The variation $\tilde{P}(H)$ for each dephased single junction is proportional to the junction effective area orthogonal to the wave vector of the electromagnetic field. For $\tilde{P}(H)$ we have

$$\tilde{P}(H) = N(T) \int_0^\infty dY l Y f(Y) (1 - e^{-(H-H_1)/H_d}), \quad (1)$$

where Y and l are, respectively, the junction length and thickness, $N(T)$ is the number of junctions for $H=0$ at the temperature T , and $f(Y)$ is the distribution function of Y chosen as the sum of two Gaussians centered, respectively, around the mean value w and $-w$, with the same variance σ .⁷

A least-squares fit of the experimental data (some of which are reported as dots in Figs. 2) gives the values of the parameters H_d and H_1 at each temperature. By inserting the values of H_d and H_1 in Eq. (1) the continuous lines of Fig. 2 are obtained. In Fig. 5 the values H_d

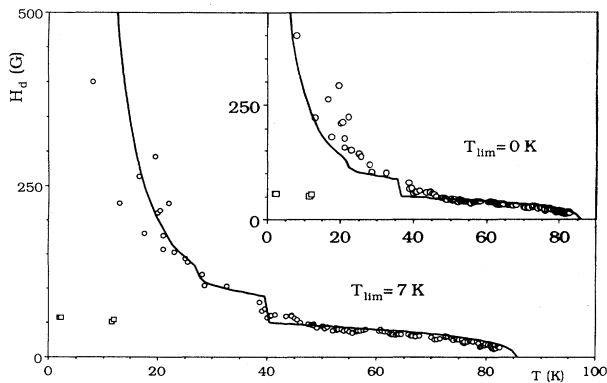


FIG. 5. Behavior of the dephasing magnetic field H_d as a function of temperature T : (○, □) refer to experimental results (□ is the first run measurement after ZFC), the solid line is the result of the fit of Sec. III C. Below ~ 45 K the measures are scattered because of metastability effects. The fit parameters are the same as in Fig. 3 with $T_{lim} = 7$ K. In the inset the continuous line refers to $T_{lim} = 0$ K.

versus T are shown (dots). In this paper, the field H_d is numerically different from that considered in (I). This is because here we assume an independent junction dephasing model by which the absorbed power $P(H)$ and the fit parameter H_d are deduced, while in paper (I) an empirical expression for $P(H)$ was assumed. H_1 values are small and lie in the range 5–10 G.

The parameter H_d can characterize the metastability effects. In the (8–45) K temperature range, the measured values of H_d depend on the maximum value of H reached in the previous run, and on the elapsed time between two consecutive measurements. At very low temperatures (the measurements have been carried out at 2.3 K), if the magnetic field H is driven up to 1 kG in the first run after ZFC, the absorbed power is insensitive to variation of H in the successive runs. In Fig. 5 the first run H_d values are indicated by squares.

B. Calculation of ΔP_0 versus T

The calculation of ΔP_0 follows from Eq. (1) when the T dependence is made explicit in it. In order to do this, taking into account that the phenomenon presents a critical temperature T_{cj} at $H=0$, we use the energy of a coupled junction

$$E_J(T, H) = \frac{\hbar}{2e} F(T) I_0 \left| \frac{\sin \pi \Phi / \Phi_0}{\pi \Phi / \Phi_0} \right|. \quad (2)$$

In Eq. (2) $\Phi_0 = ch/2e$ is the flux quantum and $F(T)$ is a function of the temperature, which in the Ambegaokar-Baratoff¹³ theory is given by

$$F(T) = \frac{\Delta(T)}{\Delta(0)} \tanh \frac{\Delta(T)}{2k_B T}, \quad (3)$$

with $\Delta(T)$ the temperature-dependent gap parameter, and $\Delta(0)$ the gap at $T=0$; I_0 is the maximum Josephson current given by

$$I_0 = \frac{\pi \Delta(0)}{e R_{ij}}, \quad (4)$$

with R_{ij} the normal-state resistance of the junction between i and j grains; $\Phi = HA$, and $A = (l + 2\lambda_g)Y$ is the effective field-penetrated junction area orthogonal to H , with $\lambda_g = \lambda_0 [F(T)]^{-1/2}$ the field penetration length in the grain. In Eq. (1) the contribution to the microwave absorbed power is given by those junctions for which the condition

$$E_J(H, T, Y) < k_B T \quad (5)$$

is fulfilled.

The best fit is given in Fig. 3 (solid line) with the values for the parameters $w = 1.6 \mu\text{m}$, $l = 0.01 \mu\text{m}$, $\lambda_0 = 0.1 \mu\text{m}$, $\sigma = 0.28 \mu\text{m}$, and with $F(T) = F_1(T)$ of paper (I). As can be seen, there is a good agreement with the experimental data above ~ 45 K. The lack of agreement at low temperatures may be attributed to the metastability effects not taken into account in Eq. (2), which is deduced from a single junction model. The temperature T_{cj} obtained by means of the equation

$$\langle E_J(T_{CJ}, 0) \rangle = \frac{\hbar}{2e} F(T_{CJ}) \langle I_0 \rangle = k_B T_{CJ} \quad (6)$$

is $T_{CJ} = 85.7$ K (Fig. 3). In Eq. (6) the brackets have the meaning

$$\langle \dots \rangle = \int_0^{+\infty} dY G_w \dots + \int_0^{+\infty} dY G_{-w} \dots,$$

where G_w and G_{-w} are two Gaussian distributions centered, respectively, around the mean values w and $-w$.

C. Behavior of the dephasing field H_d versus T

The fit of $H_d(T)$ has been obtained by means of (i) the equation

$$\langle E_J(H_d, T) \rangle = k_B T, \quad (7)$$

where the energy $E_J(H_d, T)$ is given by Eq. (2) and the average is carried out as in Eq. (6); (ii) the same values of the parameters w, l, λ_0, σ of the previous fit of ΔP_0 ; (iii) the function $F_1(T)$ of paper (I); and (iv) the introduction of a limit temperature $T_{\text{lim}} \neq 0$.

It should be stressed that in the single-junction model the dephasing field H_d diverges at zero temperature, that is $T_{\text{lim}} = 0$. However, at low temperatures superconducting-glass effects are present in these samples (as will be discussed in the following), which lead to the existence of a $T_{\text{lim}} \neq 0$. Therefore we have introduced the term T_{lim} in Eq. (7) as a fit parameter. The H_d curve of Fig. 5 is obtained with $T_{\text{lim}} = 7$ K. In the inset of this figure the same fit is reported with $T_{\text{lim}} = 0$ for comparison. In Fig. 5 the H_d values at low temperatures (\square) are those obtained in the first run in H after the ZFC. We note the good agreement between the experimental points and the fitted curves of Fig. 5 for the temperature range 45–90 K.

IV. SUPERCONDUCTING-GLASS (SG) MODEL

In paper (I) the analysis of the experimental data was carried out by means of single-junction energy, in other words assuming the junctions to be independent. However, such a simple model is not able to explain some results, among others, the existence of a well-defined temperature T_{CJ} (Fig. 3). We have said in paper (I) that T_{CJ} is connected to the model proposed by Shih, Ebner, and Stroud in granular superconductors.⁹ A SG hypothesis was suggested for high- T_c superconductors since its discovery by Muller *et al.*² and a quantitative analysis with a Monte Carlo simulation in arrays of JJ's was developed by Morgenstern *et al.*¹⁰ A system of JJ's in a network of superconductor coupled filaments have been analyzed as a SG model by Vinokur *et al.*¹¹ They showed that when the superconductor wires are placed in a magnetic field a transition to a low-temperature state of the SG type occurs. They found the dependence of the phase transition temperature $T_c(H)$ on the magnetic field H . A phase transition in a disordered granular superconductor was also considered by John and Lubensky.¹²

All these models show that, when disorder is present, there is a phase diagram in the H, T plane, related to the transition phase coherence \rightarrow noncoherence in the JJ

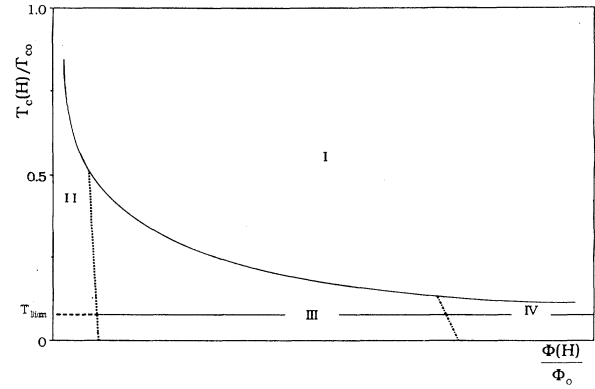


FIG. 6. Sketch of a qualitative diagram $T_c(H)$ as proposed by the authors of Refs. 9–12. T_{c0} is the bulk superconducting transition temperature of the sample. T_{CJ} is the dephasing temperature of junction arrays at zero magnetic field. T_{lim} is the asymptotic limit for $T_c(H)$. I is the dephased zone, II is the ferrocoherent zone, III is the rearranging SG zone, and IV is the frozen SG zone.

arrays or, in other words, the transition superconductor \rightarrow normal in the intrajunction zones. However, in these models there is a restriction; they assume that in the known coupling Hamiltonian

$$H = - \sum_{ij} J_{ij} \cos \left[\phi_i - \phi_j - \int_i^j \mathbf{A} \cdot d\mathbf{l} \right],$$

the coupling energy J_{ij} is the same for each junction, and independent from the temperature T and the field H .

The phase diagram, proposed by previously cited authors, i.e., the curve of the transition temperature T_c versus H , is qualitatively sketched in Fig. 6. In this figure zone I is the normal zone or dephasing zone; zone II is the ferrocoherence zone, in which the magnetic field is so low that the disorder is not able to create the SG phase; zones III and IV are the SG zones. In zone IV the arrays are completely randomly oriented and frozen, and the magnetic field is ineffective.¹⁰ For high values of H , $T_c(H)$ tends to a limiting temperature T_{lim} , as expected

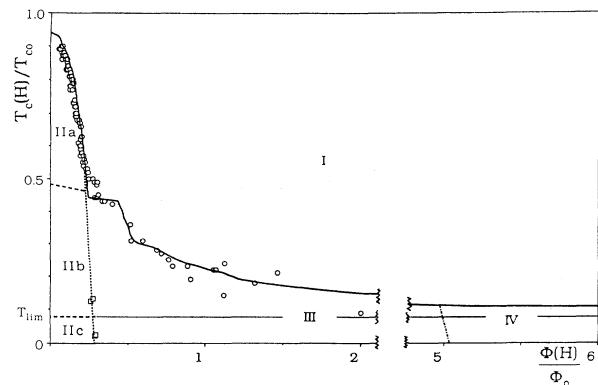


FIG. 7. The figure shows the results of Fig. 5 interpreted following the outline of Fig. 7 as explained in the text.

by Shih *et al.*⁹ and analytically calculated by Vinokur *et al.*¹¹

Now, if one considers that in our model H_d is the crossover field between coherent phase and noncoherent phase, it is possible to enclose our experimental results within the frame of the SG model in a straightforward way simply by exchanging the axes in Fig. 5. This is shown in Fig. 7, where the set of the data can be interpreted by the outline of Fig. 6 in the following way.

Considering that in our measurements the transition between different zones occurs on straight lines parallel to the H axis, the T axis has been divided in three parts. For $T/T_{c0} > 0.5$ the curves P versus H (Fig. 2) does not depend on past history, so that the value H_d is well defined. The transition II A \rightarrow I is explained in a model of independent junctions (I) and it represents the ferrocoherence \rightarrow noncoherence transition. In the range 0.5–0.08 metastability effects are present, and the values H_d depend on the past history of the sample, in particular at $T/T_{c0} = 0.14$, where one obtains the measures indicated by squares in the first run in H after ZFC and the measures indicated by circles in successive runs. For $T/T_{c0} < 0.08$ after the first run in H in ZFC, the effect is no more detectable (see curve *b* of Fig. 4) when $\Phi(H)/\Phi_0$ is larger than 5. We find the same results repeating the measurements after some hours and if the direction of H

is reversed. Curve *a* of Fig. 4 is again reproduced if the sample is heated above 45 K and then recooled at 2.3 K. Thus, when the representative point of the sample state is in the zone IV, the system is frozen; this fact supports a SG interpretation. The dashed line in Fig. 7 refers to the transition between the ferrocoherence (zone II) and the SG phase (zone III). The dashed-dotted line is related to the transition into the frozen zone (IV) and is obtained considering the minimum magnetic field at which the low-field effect disappears (see Fig. 4).

V. CONCLUSIONS

The measurements presented in this paper and in the previous one (I) show that the microwave absorption in sintered $\text{YBa}_2\text{Cu}_3\text{O}_7$ samples at low magnetic fields (< 500 G) can be explained by means of a model of arrays of Josephson junctions. When the temperature is higher than ~ 45 K both the dephasing field H_d and the maximum variation of the absorbed power ΔP_0 , as a function of the temperature T , allow us to say that the single-junction model is a good approximation. For $T < 45$ K the metastability effects and the existence of a limit temperature T_{lim} , below which the system is brought in a frozen state, suggest an interpretation in terms of a superconducting-glass model.

¹J. G. Bednorz and K. A. Müller, *Z. Phys. B* **64**, 188 (1986).

²K. A. Müller, M. Takashiga, and J. G. Bednorz, *Phys. Rev. Lett.* **58**, 1143 (1987).

³S. Sridhar, C. A. Shiffman, and H. Hamdeh, *Phys. Rev. B* **36**, 2301 (1987); K. W. Blazey, K. A. Müller, J. G. Bednorz, W. Berlinger, G. Amoretti, E. Buluggiu, A. Vera, and F. C. Matocotta, *ibid.* **36**, 7241 (1987); A. M. Portis, K. W. Blazey, K. A. Müller, and J. G. Bednorz, *Europhys. Lett.* **5**, 467 (1988); A. T. Wijeratne, G. L. Dunifer, J. T. Chen, L. E. Wenger, and E. M. Logothetis, *Phys. Rev. B* **37**, 615 (1988); K. Khachatryan, E. R. Weber, P. Tejedor, A. M. Stacy, and A. M. Portis, *ibid.* **36**, 8309 (1987); M. Peric, B. Rakvin, M. Prester, N. Brnicevic, and A. Dulcic, *ibid.* **37**, 522 (1988).

⁴R. Fastampa, M. Giura, R. Marcon, and C. Matocotta, *Europhys. Lett.* **6**, 265 (1988).

⁵Y. Yeshurun and A. P. Malozemoff, *Phys. Rev. Lett.* **60**, 2202 (1988); M. Tinkham, *ibid.* **61**, 1658 (1988); J. Mannhart, P. Chaudhari, D. Dimos, C. C. Tsuei, and T. R. McGuire, *ibid.*

61, 2476 (1988); T. T. M. Paltstra, B. Battlogg, L. F. Schneemeyer, and J. V. Waszczak, *ibid.* **61**, 1662 (1988).

⁶C. Giovannella, G. Collin, and I. A. Campbell, *J. Phys. (Paris)* **48**, 1835 (1987).

⁷R. Marcon, R. Fastampa, M. Giura, and C. Matocotta, *Phys. Rev. B* **39**, 2796 (1989).

⁸S. H. Glarum, J. H. Marshall, and L. F. Schneemeyer, *Phys. Rev. B* **37**, 7491 (1988).

⁹W. Y. Shih, C. Ebner, and D. Stroud, *Phys. Rev. B* **30**, 134 (1984).

¹⁰I. Morgenstern, K. A. Müller, and J. G. Bednorz, *Z. Phys. B* **69**, 33 (1987-88).

¹¹V. M. Vinokur, L. B. Ioffe, A. I. Larkin, and M. V. Feigel'man, *Zh. Eksp. Teor. Fiz.* **93**, 343 (1987) [*Sov. Phys.—JETP* **66**, 198 (1987)].

¹²S. John and T. C. Lubensky, *Phys. Rev. B* **34**, 4815 (1986).

¹³V. Ambegaokar and A. Baratoff, *Phys. Rev. Lett.* **10**, 486 (1963); **11**, 104 (1963).